Supporting Information for：

Theoretical investigation on the atmospheric degradation mechanism, kinetics, and fate of hydroxymethyl nitrate initiated by ·OH radical

Xiang-Huan Liu[a], Ting-Ting Meng[a], Feng-Yang Bai[a*], Shuang Ni[a*], Zhen Zhao[a,b*]

[a]*Institute of Catalysis for Energy and Environment, College of Chemistry and Chemical Engineering, Shenyang Normal University, Shenyang, 110034, People's Republic of China*

[b]*State Key Laboratory of Heavy Oil Processing, China University of Petroleum, Chang Ping, Beijing 102249, People's Republic of China*

*Corresponding author: baify492@nenu.edu.cn (Feng-Yang Bai)
*Corresponding author: nis223@nenu.edu.cn (Shuang Ni)
*Corresponding author: zhenzhao@cup.edu.cn (Zhen Zhao)

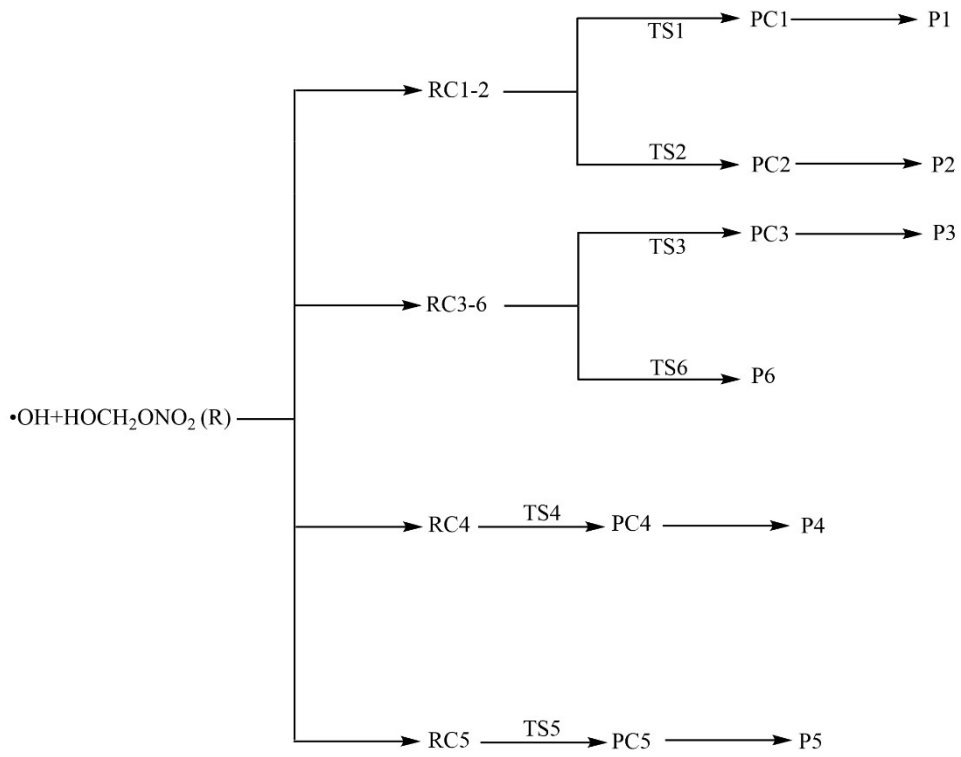

Figure S1. The reactions routes of $HOCH_2ONO_2$ mediated by the ·OH radical.

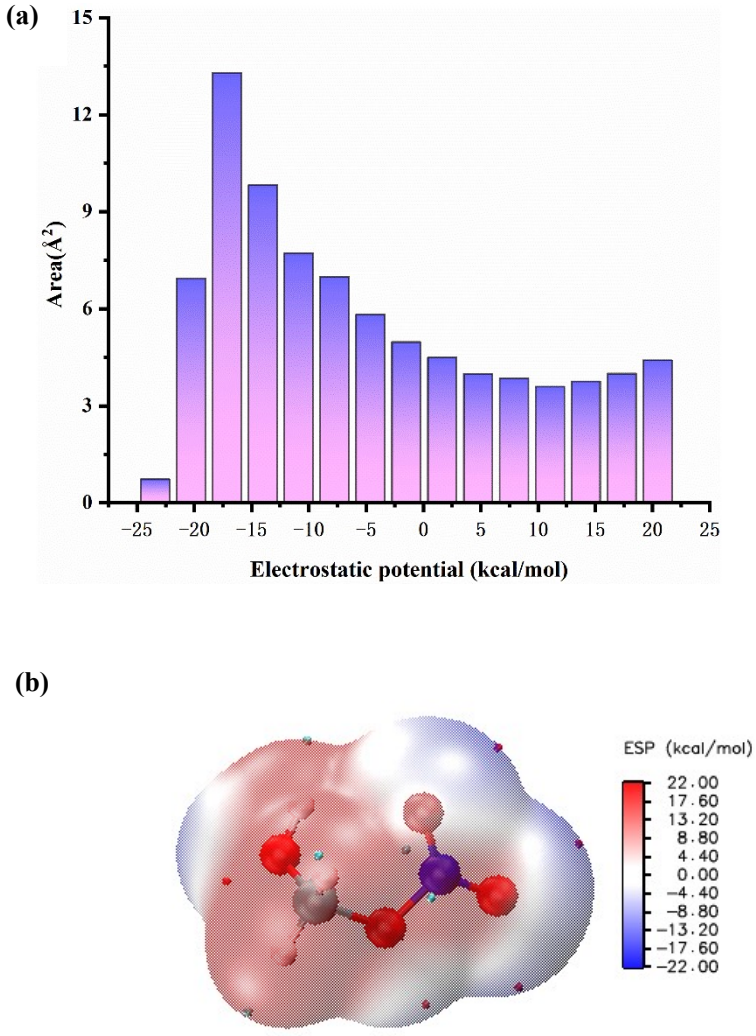

Figure S2. The electrostatic potential on the surface of $HOCH_2ONO_2$ molecule and its bar graph.

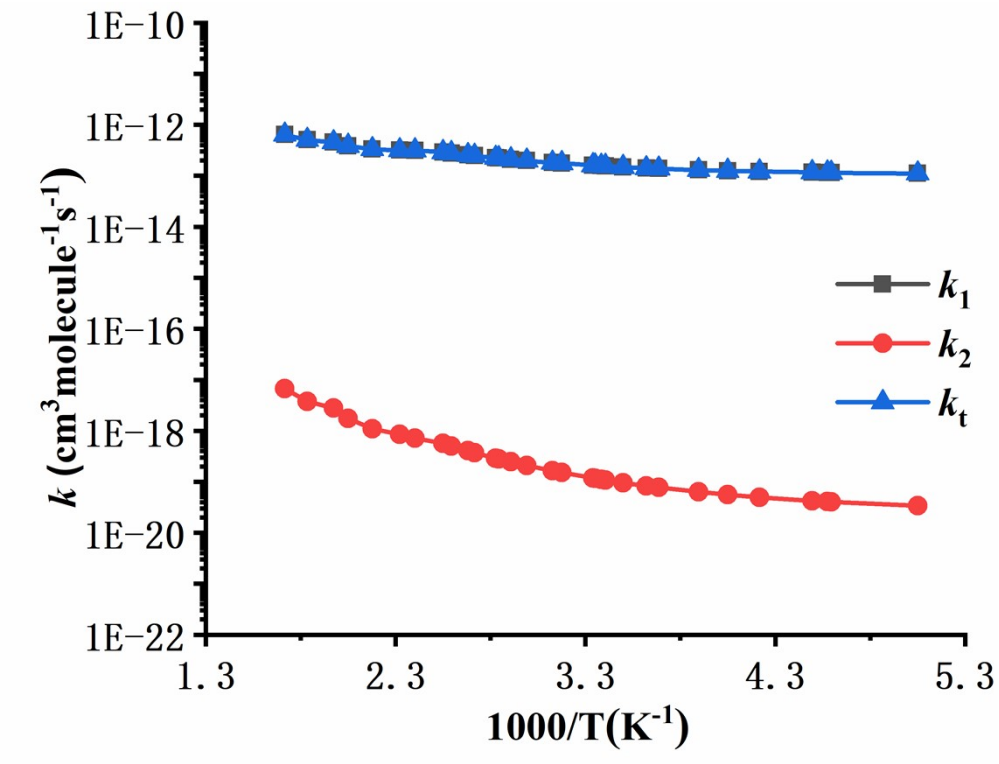

Figure S3. Plots of calculated individual and overall CVT/SCT rate constants (k_1, k_2, and k_t) as a function of 1000/T.

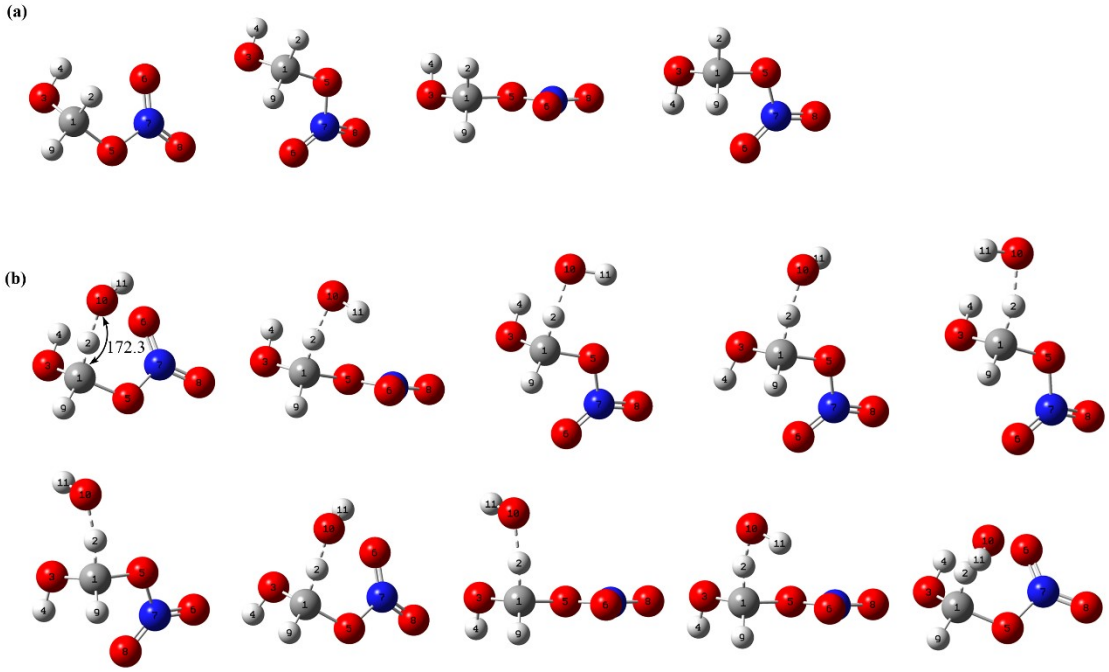

Figure S4. Geometric conformations of reactants and transition states optimized at the M06-2X/6-311+G(d,p) level.

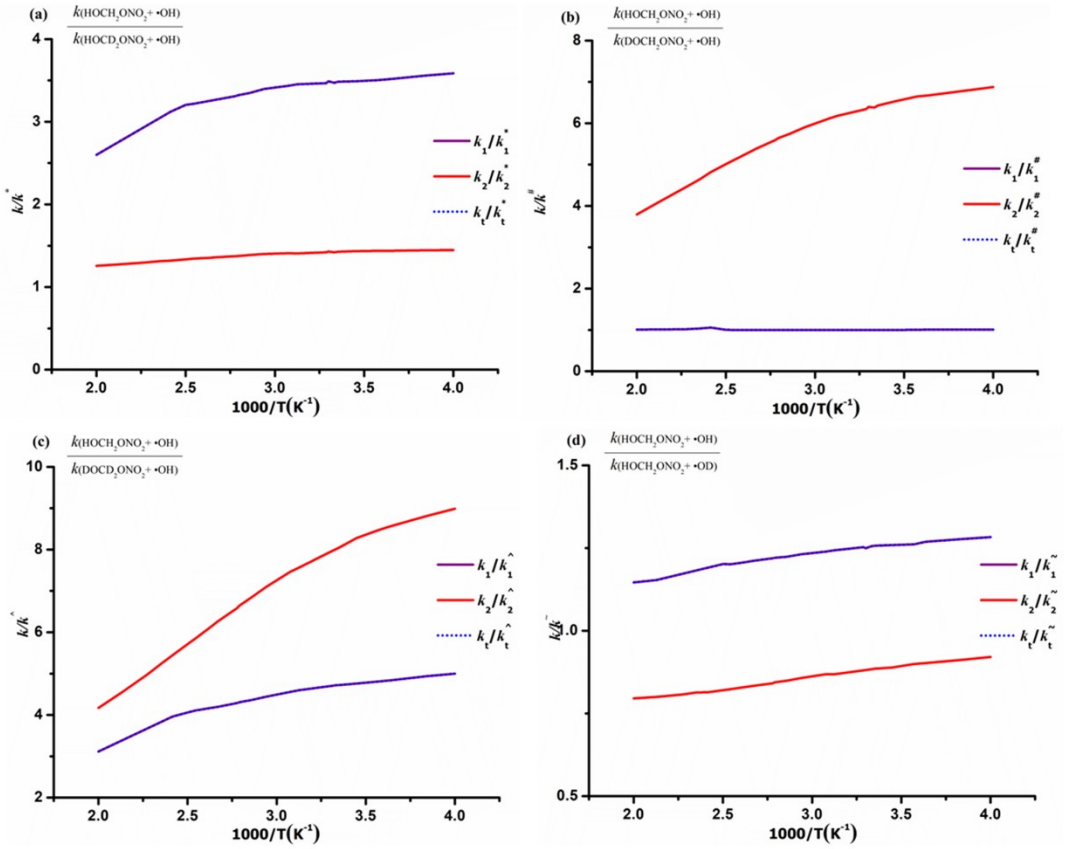

Figure S5. The k_H/k_D for the reactions of $HOCH_2ONO_2/HOCD_2ONO_2$ + OH (R*) (a), $HOCH_2ONO_2/DOCH_2ONO_2$ + OH ($R^{\#}$) (b), $HOCH_2ONO_2/DOCD_2ONO_2$ + OH ($R^{\wedge}$) (c), and $HOCH_2ONO_2$ + OH/OD ($R^{\sim}$) (d).

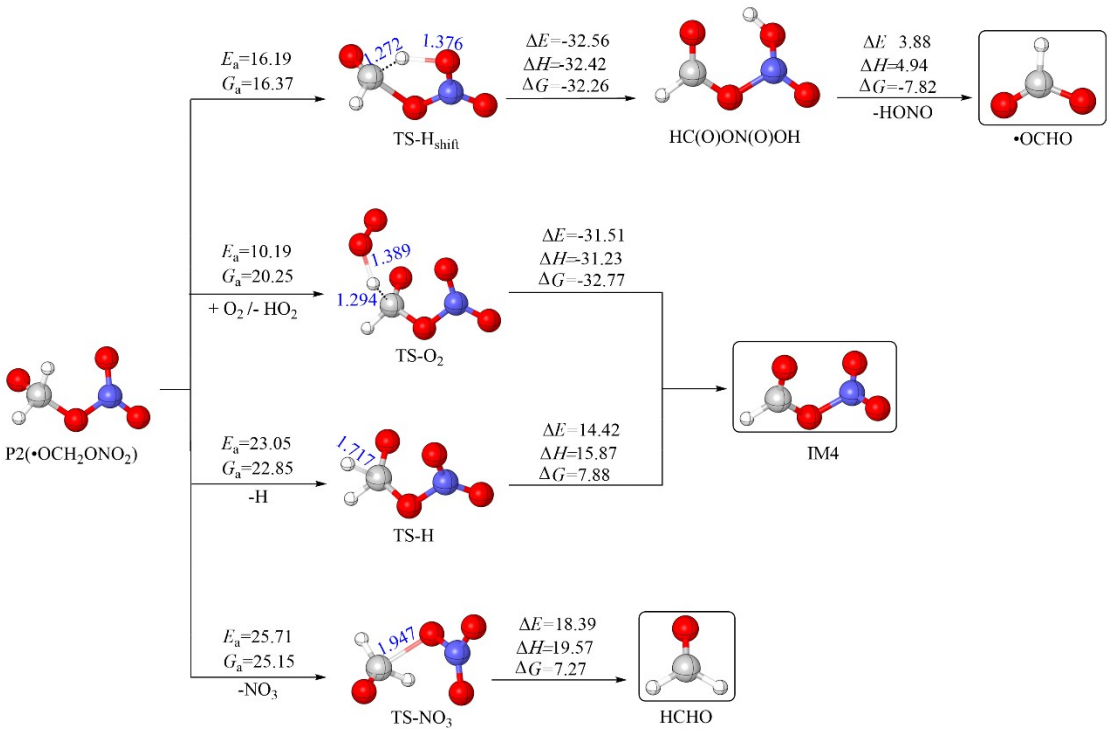

Figure S6. The degradation routes of ·OCH_2ONO_2 (P2) and the corresponding geometries (Bond length: Å) along with the activation energy (E_a), activation Gibbs free energy (G_a), relative energies (ΔE), enthalpy (ΔH), and Gibbs free energy (ΔG) of the transformation processes at the M06-2X/6-311+G(d,p) level.

.

Table S1. Computed relative energies (Δ*E*) including ZPE corrections, enthalpy (Δ*H*), and Gibbs free energy (Δ*G*) for species involved reaction of ·OH radical with $HOCH_2ONO_2$ at the CCSD(T)/aug-cc-pVDZ, CCSD(T)/aug-cc-pVTZ, and CCSD(T)/CBS levels of theory based on the M06-2X/6-311+G(d,p)-optimized geometries.

Parameters / Species \ Levels	Δ*E*			Δ*H*			Δ*G*		
	DZ	TZ	CBS	DZ	TZ	CBS	DZ	TZ	CBS
R+·OH	0.0	0.0	0.0	0.0	0.0	0.0	0.0	0.0	0.0
RC1-2	-3.99	-3.99	-3.99	-4.22	-4.22	-4.22	3.24	3.25	3.25
TS1	1.35	1.39	1.44	0.56	0.60	0.64	9.58	9.62	9.66
PC1	-18.69	-19.97	-21.27	-18.34	-19.62	-20.92	-11.71	-12.98	-14.28
P1+H_2O	-16.00	-17.79	-19.61	-15.60	-66.66	-19.22	-16.93	-67.99	-20.54
TS2	17.31	16.20	15.06	16.48	15.37	14.23	25.67	24.56	23.42
PC2	-13.45	-13.72	-13.99	-13.32	-13.58	-13.86	-6.73	-7.00	-7.27
P2+H_2O	-10.30	-10.73	-11.17	-10.00	-59.70	-10.87	-11.35	-61.05	-12.22
RC3-6	-3.10	-2.72	-2.32	-3.12	-2.73	-2.34	3.84	4.23	4.62
TS3	23.73	25.46	27.23	23.48	25.21	26.98	31.14	32.87	34.63
PC3	-3.12	-4.26	-5.42	-2.94	-4.08	-5.24	3.38	2.25	1.08
P3+NO_2	-0.27	-2.01	-3.79	-0.41	-2.14	-3.92	-3.18	-4.92	-6.70
RC4	-2.57	-2.49	-2.41	-2.86	-2.78	-2.70	4.43	4.51	4.59
TS4	36.87	38.02	39.21	36.32	37.48	38.67	44.87	46.03	47.21
PC4	-10.01	-9.93	-9.85	-10.02	-9.94	-9.86	-3.34	-3.26	-3.18
P4+NO_3	-6.19	-6.82	-7.46	-6.57	-7.20	-7.84	-9.27	-9.90	-10.54
RC5	-2.78	-2.37	-1.96	-2.95	-2.55	-2.14	4.94	5.35	5.76
TS5	27.50	29.88	32.32	26.52	28.91	31.35	36.55	38.94	41.38
PC5	-10.92	-11.69	-12.48	-11.00	-11.77	-12.56	-4.12	-4.90	-5.68
P5+HNO_3	-6.25	-7.57	-8.91	-6.62	-207.70	-9.29	-9.34	-210.41	-12.01
TS6	33.29	33.87	34.47	31.97	32.55	33.14	42.50	43.08	43.68
P6	30.89	30.31	29.72	29.67	29.09	28.50	40.08	39.50	38.91

Table S2. The values of variational and tunneling transmission coefficients for the major channel RP1 of ·OH radical with $HOCH_2ONO_2$ in the temperature range of 200—600 K.

T (K)	*TST/CVT*	*(CVT/SCT)/CVT*
200	1.67	23.11
220	1.51	14.95
221	1.50	14.60
225	1.48	13.52
240	1.39	10.39
250	1.35	8.87
260	1.31	7.69
275	1.26	6.34
280	1.24	5.98
290	1.22	5.37
298	1.20	4.95
300	1.19	4.86
303	1.19	4.72
304	1.18	4.68
320	1.15	4.08
325	1.14	3.91
340	1.12	3.49
350	1.10	3.27
358	1.10	3.10
360	1.09	3.04
375	1.08	2.79
380	1.07	2.71
393	1.05	2.53
400	1.05	2.45
414	1.03	2.27
425	1.03	2.03
440	1.02	1.83
470	1.01	1.58
500	1.01	1.42
520	1.01	1.34
560	1.00	1.23
600	1.00	1.14

Table S3. Branching ratios of k_1/k_t and k_2/k_t at 200−600 K.

T (K)	k_1/k_t	k_2/k_t
200	100%	0%
220	100%	0%
221	100%	0%
225	100%	0%
240	100%	0%
250	100%	0%
260	100%	0%
275	100%	0%
280	100%	0%
290	100%	0%
298	100%	0%
300	100%	0%
303	100%	0%
304	100%	0%
320	100%	0%
325	100%	0%
340	100%	0%
350	100%	0%
358	100%	0%
360	100%	0%
375	100%	0%
380	100%	0%
393	100%	0%
400	100%	0%
414	100%	0%
425	100%	0%
440	100%	0%
470	100%	0%
500	100%	0%
520	100%	0%
560	100%	0%
600	100%	0%

Table S4. The k_H/k_D for the individual and overall reactions of $HOCH_2ONO_2/HOCD_2ONO_2$ + ·OH (R*) at 250−500 K.

T (K)	k_1/k_1^*	k_2/k_2^*	k_t/k_t^*
250	3.59	1.45	3.59
260	3.56	1.45	3.56
275	3.52	1.44	3.52
280	3.50	1.44	3.50
290	3.49	1.43	3.49
298	3.49	1.43	3.49
300	3.47	1.42	3.47
303	3.49	1.43	3.49
304	3.47	1.42	3.47
320	3.45	1.41	3.45
325	3.44	1.41	3.44
340	3.40	1.40	3.40
350	3.35	1.39	3.35
358	3.32	1.38	3.32
360	3.31	1.37	3.31
375	3.25	1.36	3.25
380	3.23	1.35	3.23
393	3.22	1.34	3.22
400	3.20	1.33	3.20
414	3.12	1.32	3.12
425	2.93	1.31	2.93
440	2.74	1.30	2.74
470	2.55	1.28	2.55
500	2.60	1.26	2.60

Table S5. The k_H/k_D for the individual and overall reactions of $HOCH_2ONO_2/DOCH_2ONO_2$ + OH ($R^{\#}$) at 250−500 K.

T (K)	$k_1/k_1^{\#}$	$k_2/k_2^{\#}$	$k_t/k_t^{\#}$
250	1.01	6.88	1.01
260	1.01	6.79	1.01
275	1.01	6.67	1.01
280	1.00	6.65	1.00
290	1.00	6.53	1.00
298	1.00	6.43	1.00
300	1.00	6.38	1.00
303	1.00	6.39	1.00
304	1.00	6.34	1.00
320	1.00	6.18	1.00
325	1.00	6.11	1.00
340	1.00	5.90	1.00
350	1.00	5.74	1.00
358	1.00	5.64	1.00
360	1.00	5.60	1.00
375	1.00	5.38	1.00
380	1.00	5.30	1.00
393	1.00	5.11	1.00
400	1.00	5.01	1.00
414	1.06	4.82	1.06
425	1.03	4.64	1.03
440	1.02	4.45	1.02
470	1.01	4.10	1.01
500	1.01	3.79	1.01

Table S6. The k_H/k_D for the individual and overall reactions of $HOCH_2ONO_2/DOCD_2ONO_2$ + OH (R^) at 250−500 K.

T (K)	$k_1/\hat{k_1}$	$k_2/\hat{k_2}$	$k_t/\hat{k_t}$
250	5.00	8.99	5.00
260	4.94	8.82	4.94
275	4.83	8.56	4.83
280	4.81	8.47	4.81
290	4.76	8.28	4.76
298	4.72	8.06	4.72
300	4.72	7.99	4.72
303	4.70	8.01	4.70
304	4.69	7.92	4.69
320	4.60	7.56	4.60
325	4.56	7.47	4.56
340	4.44	7.09	4.44
350	4.36	6.84	4.36
358	4.31	6.65	4.31
360	4.29	6.58	4.29
375	4.19	6.25	4.19
380	4.17	6.13	4.17
393	4.11	5.85	4.11
400	4.06	5.71	4.06
414	3.96	5.44	3.96
425	3.65	5.24	3.65
440	3.40	4.98	3.40
470	3.13	4.54	3.13
500	3.12	4.17	3.12

Table S7. The k_H/k_D for the individual and overall reactions of $HOCH_2ONO_2$ + OH/OD (R^-) at 250−500 K.

T (K)	$k_1/\tilde{k_1}$	$k_2/\tilde{k_2}$	$k_t/\tilde{k_t}$
250	1.28	0.92	1.28
260	1.28	0.91	1.28
275	1.27	0.90	1.27
280	1.26	0.90	1.26
290	1.26	0.89	1.26
298	1.26	0.89	1.26
300	1.26	0.88	1.26
303	1.25	0.89	1.25
304	1.25	0.88	1.25
320	1.24	0.87	1.24
325	1.24	0.87	1.24
340	1.23	0.86	1.23
350	1.22	0.85	1.22
358	1.22	0.84	1.22
360	1.22	0.84	1.22
375	1.21	0.83	1.21
380	1.21	0.83	1.21
393	1.20	0.82	1.20
400	1.20	0.82	1.20
414	1.18	0.81	1.18
425	1.12	0.81	1.12
440	1.14	0.81	1.14
470	1.15	0.80	1.15
500	1.15	0.80	1.15

Table S8. The k_H/k_D for the overall reaction of $HOCH_2ONO_2/HOCD_2ONO_2$+OH (k_t/k_t^*), $HOCH_2ONO_2/DOCH_2ONO_2$+OH ($k_t/k_t^{\#}$), $HOCH_2ONO_2/DOCD_2ONO_2$+OH ($k_t/\hat{k_t}$), and $HOCH_2ONO_2$ + OH/OD ($k_t/\tilde{k_t}$) at 250−500 K.

T (K)	k_t/k_t^*	$k_t/k_t^{\#}$	$k_t/\hat{k_t}$	$k_t/\tilde{k_t}$
250	5.00	3.59	1.01	1.28
260	4.94	3.56	1.01	1.28
275	4.83	3.52	1.01	1.27
280	4.81	3.50	1.00	1.26
290	4.76	3.49	1.00	1.26
298	4.72	3.49	1.00	1.26
300	4.72	3.47	1.00	1.26
303	4.70	3.49	1.00	1.25
304	4.69	3.47	1.00	1.25
320	4.60	3.45	1.00	1.24
325	4.56	3.44	1.00	1.24
340	4.44	3.40	1.00	1.23
350	4.36	3.35	1.00	1.22
358	4.31	3.32	1.00	1.22
360	4.29	3.31	1.00	1.22
375	4.19	3.25	1.00	1.21
380	4.17	3.23	1.00	1.21
393	4.11	3.22	1.00	1.20
400	4.06	3.20	1.00	1.20
414	3.96	3.12	1.06	1.18
425	3.65	2.93	1.03	1.12
440	3.40	2.74	1.02	1.14
470	3.13	2.55	1.01	1.15
500	3.12	2.60	1.01	1.15